Journal of Computer-Aided Molecular Design, 7 (1993) 71–82
ESCOM

J-CAMD 182

Nonlinear dependence in comparative molecular field analysis

Ki Hwan Kim

Computer Assisted Molecular Design, Pharmaceutical Products Division, Abbott Laboratories, Abbott Park, IL 60064, U.S.A.

Received 15 January 1992
Accepted 23 June 1992

Key words: 3D QSAR; Comparative molecular field analysis (CoMFA); GRID; Parabolic; Bilinear; Nonlinear; Hydrophobicity

SUMMARY

The applicability of the comparative molecular field analysis (CoMFA) approach to describe the nonlinear dependence of biological activity on lipophilicity in 3D quantitative structure-activity relationships (QSAR) has been demonstrated. The results indicate that the CoMFA approach is appropriate for describing nonlinear effects in 3D QSAR studies.

INTRODUCTION

In biological quantitative structure–activity relationships (QSAR), the biological responses elicited by drugs are usually correlated with a combination of hydrophobic, steric, and electronic properties of the molecules. It is well known that the relationships between the biological activity and the physicochemical properties of the compounds are often nonlinear. This is especially true for the hydrophobicity of drugs.

Several models have been proposed to describe such nonlinear relationships. The most often used models are the parabolic model, proposed by Hansch and Clayton [1], and the bilinear model, proposed by Kubinyi [2]. Advantages and disadvantages of these as well as other models have been discussed in the literature [3]. One limitation of these classic models is that they do not include consideration of 3D structures. In the CoMFA method [4], the model is derived from the 3D structure of the molecules by calculating the interaction energies at the 3D lattice points. The resulting correlations are displayed as a 3D coefficient contour map, thus including 3D information.

In the previous study, CoMFA methodology was used to predict the Hammett σ and pK_a's as well as some steric parameters including E_s [5–7]. We reported our findings on the parameterization of hydrophobic effects directly from 3D structures using a CoMFA approach with GRID

force field [8]. In this study we report an investigation of the applicability of CoMFA methodology on nonlinear relationships.

Eleven sets of biological data from the literature were selected to demonstrate the applicability of the CoMFA methodology in describing a nonlinear dependence in 3D QSAR. A water probe and the GRID force field [9] were used in the analysis to describe the hydrophobic effects. In order to compare the CoMFA nonlinear model with the parabolic and bilinear models, biological data that have been reported with the parabolic and bilinear models were selected.

METHODS

Molecular modeling

The starting coordinates were generated using the graphics modeling package for small molecules at Abbott or with the program CONCORD [10]. Since no information about the active conformation was available, all the alkyl substituents were chosen to be in an extended conformation. All geometric variables were optimized with AM1 of AMPAC [11]. The molecules in each set were aligned by superimposing the benzyldimethylammonium moiety.

CoMFA interaction energy calculation

The hydrophobic potential energy fields of each molecule were calculated at various lattice points surrounding the molecule using a H_2O probe group with the program GRID. A van der Waals radius of 1.70 and a charge of 0.0 were used for the H_2O probe with two hydrogen-bond-donating and two hydrogen-bond-accepting properties.

For each substituted alkylbenzyldimenthylammonium chloride molecule, the energies at a total of 3168 grid points were calculated with 2 Å spacing in a lattice of $34 \times 30 \times 20$ ($X = -17$ to 17, $Y = -14$ to 16, $Z = -9$ to 11). All energy values greater than 4.0 kcal/mol were truncated to 4.0. Any lattice point for which the standard deviation of the energies was less than 0.05 was discarded. These procedures reduced the number of lattice points to 175, 183, 173, 173, 187, 187, 187, 187, 178, 173, and 178 for Eqs. 1A–11A, respectively. The Cartesian coordinates of a nonadecyl analogue are given in the Appendix as a reference compound.

Partial least-squares (PLS) calculations

Seven or less orthogonal latent variables were first extracted by the standard PLS algorithm [12]. The number of latent variables extracted was always at least 3 less than the number of the compounds included in the correlation. These latent variables were subjected to the PLS cross-validation test [12,13] in the original order of extraction or in the order of their correlation with the dependent variable. The 'best' correlation model was chosen on the basis that it significantly minimized the sum of squares of the difference in activity between the predicted and observed values using predictions made from a leave-one-out jackknife validation test. After the number of latent variables was established, the 'best' correlation model was derived. The final model was further validated by the overall and the stepwise F-statistics. If F-statistics did not support the model, the least significant latent variable was eliminated and the model was rederived. The

variables $Z1_{H_2O}$ and $Z2_{H_2O}$ in the correlation equations are the first and second latent variables from a H_2O probe obtained from the PLS analysis of each example.

RESULTS

Equations 1–11 were derived from log MIC or log MKC values of the 6 to 12 $C_6H_5CH_2N^+R(CH_3)_2\ Cl^-$ compounds in Table 1. The alkyl groups in the compounds included are C_9H_{19}–$C_{19}H_{39}$. MIC or MKC in Eqs. 1–11 is the measured minimum inhibitory concentration or minimum killing concentration of the benzyldimethylalkylammonium compounds against various microbial strains. The measured activity data were originally reported by Cutler et al. [14].

Equations 1A–11A in Table 2 are the nonlinear correlations obtained using the CoMFA method. The corresponding correlations from parabolic [1] (Eqs. 1B–11B) and bilinear [15] model (Eqs. 1C–11C) are given along with those from the CoMFA model:

(1A–11A) CoMFA: $\text{Log BA} = a\ Z1_{H_2O} + bZ2_{H_2O} + c.$

(1B–11B) Parabolar: $\text{Log BA} = a \log P + b\ (\log P)^2 + c.$

(1C–11C) Bilinear: $\text{Log BA} = a \log P + b \log (\beta P+1) + c.$

In the correlation equations, n is the number of compounds used in the correlation, s is the residual standard error of estimate, r is the correlation coefficient, and press s is the standard error of estimate from the leave-one-out jackknife cross-validation.

Equations 1–11 show that the variance in the log MIC or log MKC values of these compounds can be explained by their lipophilic character. The quality of the correlations from the CoMFA

TABLE 1
OBSERVED AND CALCULATED LOG MIC AND LOG MKC VALUES USING EQS. 1A–11A

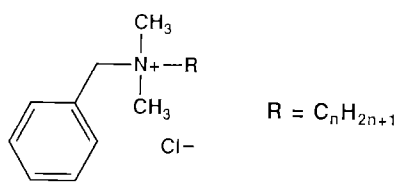

No.	Subst.	Obs.	Calc.	Dev.	$Z1_{H_2O}$	$Z2_{H_2O}$
P. aeruginosa. Log MIC: Eq. 1A						
1	C_9H_{19}	2.54	2.520	0.020	−10.0680	3.8280
2	$C_{10}H_{21}$	2.57	2.692	−0.122	−7.2930	4.5010
3	$C_{11}H_{23}$	3.06	2.981	0.079	−2.9140	6.9420
4	$C_{12}H_{25}$	3.48	3.399	0.081	3.7590	8.9020
5	$C_{13}H_{27}$	3.50	3.514	−0.014	6.0660	7.1790
6	$C_{14}H_{29}$	3.52	3.493	0.027	6.6230	2.7810
7	$C_{15}H_{31}$	3.14	3.304	−0.164	4.8230	−3.9780
8	$C_{18}H_{37}$	2.89	2.876	0.014	−0.2420	−14.4940
9	$C_{19}H_{39}$	2.91	2.832	0.078	−0.7560	−15.6600

TABLE 1 (continued)

No.	Subst.	Obs.	Calc.	Dev.	$Z1_{H_2O}$	$Z2_{H_2O}$
S. typhosa. Log MIC: Eq. 2A						
1	C_8H_{17}	3.52	3.481	0.039	−13.7880	−3.4000
2	C_9H_{19}	3.72	3.625	0.095	−11.9140	−2.1400
3	$C_{10}H_{21}$	3.74	3.857	−0.117	−8.5870	−0.4510
4	$C_{11}H_{23}$	4.06	4.136	−0.076	−5.1000	2.1940
5	$C_{12}H_{25}$	4.61	4.588	0.022	0.7230	6.2550
6	$C_{13}H_{27}$	4.80	4.772	0.028	3.9150	6.9140
7	$C_{14}H_{29}$	4.82	4.845	−0.025	6.9260	5.0250
8	$C_{15}H_{31}$	4.84	4.789	0.051	9.0860	0.9910
9	$C_{16}H_{33}$	4.68	4.681	−0.001	9.7220	−2.4700
10	$C_{19}H_{39}$	4.21	4.225	−0.015	9.0170	−12.9160
P. vulgaris. Log MIC: Eq. 3A						
1	C_9H_{19}	2.54	2.530	0.010	−13.5330	−3.5870
2	$C_{10}H_{21}$	2.74	2.752	−0.012	−10.9810	−1.2970
3	$C_{11}H_{23}$	3.06	3.059	0.001	−7.4400	1.8550
4	$C_{12}H_{25}$	3.61	3.564	0.046	−1.2230	6.6050
5	$C_{13}H_{27}$	3.80	3.763	0.037	2.0720	7.5110
6	$C_{14}H_{29}$	3.65	3.828	−0.178	4.9490	5.7800
7	$C_{15}H_{31}$	3.84	3.796	0.044	7.1390	2.5640
8	$C_{16}H_{33}$	3.68	3.681	−0.001	7.6570	−0.7050
9	$C_{17}H_{35}$	3.57	3.425	0.145	6.8280	−5.7200
10	$C_{19}H_{39}$	2.91	3.001	−0.091	4.5320	−13.0050
P. vulgaris. Log MKC: Eq. 4A						
1	C_9H_{19}	2.54	2.531	0.009	−7.9500	9.4330
2	$C_{10}H_{21}$	2.74	2.753	−0.013	−5.6290	8.9850
3	$C_{11}H_{23}$	3.06	3.061	−0.001	−2.4140	8.5420
4	$C_{12}H_{25}$	3.61	3.576	0.034	3.0120	7.1430
5	$C_{13}H_{27}$	3.80	3.779	0.021	5.3160	4.7150
6	$C_{14}H_{29}$	3.65	3.841	−0.191	−6.3220	0.4800
7	$C_{15}H_{31}$	3.84	3.764	0.076	5.8110	−2.7030
8	$C_{16}H_{33}$	3.68	3.576	0.104	4.1140	−5.4780
9	$C_{18}H_{37}$	2.71	2.757	−0.047	−3.5190	−14.7090
10	$C_{19}H_{39}$	2.60	2.592	0.008	−5.0620	−16.4090
S. aureus. Log MIC: Eq. 5A						
1	C_8H_{17}	3.69	3.748	−0.058	−15.9100	−5.5870
2	C_9H_{19}	4.02	4.058	−0.038	−13.5410	−3.0780
3	$C_{10}H_{21}$	4.74	4.619	0.121	−9.2190	1.4090
4	$C_{11}H_{23}$	5.06	5.033	0.027	−5.6810	4.3930
5	$C_{12}H_{25}$	5.61	5.607	0.003	−0.2800	8.0030
6	$C_{13}H_{27}$	5.80	5.823	−0.023	2.5860	8.5200
7	$C_{14}H_{29}$	5.82	5.894	−0.074	5.2870	6.9200

TABLE 1 (continued)

No.	Subst.	Obs.	Calc.	Dev.	$Z1_{H_2O}$	$Z2_{H_2O}$
S. aureus. Log MIC: Eq. 5A						
8	$C_{15}H_{31}$	5.84	5.779	0.061	7.2020	3.1690
9	$C_{16}H_{33}$	5.56	5.589	−0.029	7.7510	−0.3820
10	$C_{17}H_{35}$	5.18	5.258	−0.078	7.4960	−5.3640
11	$C_{18}H_{37}$	5.19	5.065	0.125	7.2570	−8.1670
12	$C_{19}H_{39}$	4.91	4.946	−0.036	7.0530	−9.8370
Cl. welchii. Log MIC: Eq. 6A						
1	C_8H_{17}	3.00	2.900	0.100	−15.7710	−5.8120
2	C_9H_{19}	3.02	3.116	−0.096	−14.1220	−4.3190
3	$C_{10}H_{21}$	3.57	3.600	−0.030	−10.7760	−0.6110
4	$C_{11}H_{23}$	4.06	4.033	0.027	−7.6570	2.5860
5	$C_{12}H_{25}$	4.61	4.676	−0.066	−2.5760	6.8310
6	$C_{13}H_{27}$	5.10	4.990	0.110	0.5940	8.1570
7	$C_{14}H_{29}$	5.12	5.160	−0.040	4.0100	7.0340
8	$C_{15}H_{31}$	5.14	5.166	−0.026	7.1180	3.7550
9	$C_{16}H_{33}$	5.16	5.082	0.078	8.7170	0.7530
10	$C_{17}H_{35}$	4.70	4.834	−0.134	9.6910	−4.0720
11	$C_{18}H_{37}$	4.71	4.704	0.006	10.2160	−6.6100
12	$C_{19}H_{39}$	4.73	4.657	0.073	10.5570	−7.6930
P. aeruginosa. Log MKC: Eq. 7A						
1	C_8H_{17}	1.68	1.697	−0.017	−14.3990	−2.9470
2	C_9H_{19}	2.08	1.987	0.093	−12.0860	−0.9500
3	$C_{10}H_{21}$	2.41	2.475	−0.065	−8.0500	2.1990
4	$C_{11}H_{23}$	2.92	2.916	0.004	−4.3530	4.9940
5	$C_{12}H_{25}$	3.45	3.549	−0.099	1.2910	8.5360
6	$C_{13}H_{27}$	3.85	3.821	0.029	4.2350	9.3480
7	$C_{14}H_{29}$	3.96	3.894	0.066	6.4660	7.6240
8	$C_{15}H_{31}$	3.74	3.683	0.057	7.1780	2.9340
9	$C_{16}H_{33}$	3.30	3.405	−0.105	6.7350	−1.3680
10	$C_{17}H_{35}$	3.06	2.980	0.080	5.3290	−6.9760
11	$C_{18}H_{37}$	2.63	2.668	−0.038	4.0920	−10.8020
12	$C_{19}H_{39}$	2.52	2.526	−0.006	3.5620	−12.5920
Cl. welchii. Log MKC: Eq. 8A						
1	C_8H_{17}	2.69	2.715	−0.025	−15.9660	−6.4070
2	C_9H_{19}	3.02	3.016	0.004	−14.0860	−4.1710
3	$C_{10}H_{21}$	3.57	3.560	0.010	−10.6380	−0.1930
4	$C_{11}H_{23}$	4.06	4.018	0.042	−7.5260	2.9390
5	$C_{12}H_{25}$	4.61	4.682	−0.072	−2.5080	6.9310
6	$C_{13}H_{27}$	5.10	5.002	0.098	0.6100	8.0910
7	$C_{14}H_{29}$	5.12	5.172	−0.052	3.9840	6.8670
8	$C_{15}H_{31}$	5.14	5.175	−0.035	7.0670	3.5680

TABLE 1 (continued)

No.	Subst.	Obs.	Calc.	Dev.	$Z1_{H_2O}$	$Z2_{H_2O}$
Cl. welchii. Log MKC: Eq. 8A						
9	$C_{16}H_{33}$	5.16	5.087	0.073	8.6610	0.6000
10	$C_{17}H_{35}$	4.70	4.833	−0.133	9.6610	−4.0760
11	$C_{18}H_{37}$	4.71	4.700	0.010	10.1990	−6.5430
12	$C_{19}H_{39}$	4.73	4.651	0.079	10.5420	−7.6070
Red cell sheep. Log $C_{H_{50}}$: Eq. 9A						
1	C_8H_{17}	1.52	1.615	−0.095	−15.8230	−6.8530
2	$C_{10}H_{21}$	3.45	3.244	0.206	−8.5620	3.3970
3	$C_{12}H_{25}$	4.34	4.391	−0.051	−1.0670	7.4320
4	$C_{14}H_{29}$	4.63	4.777	−0.147	4.6890	4.4400
5	$C_{16}H_{33}$	4.88	4.827	0.053	9.5080	−1.4250
6	$C_{18}H_{37}$	4.60	4.565	0.035	11.2560	−6.9910
C. albicans. Log MKC: Eq. 10A						
1	C_9H_{19}	2.54	2.594	−0.054	−13.9490	−3.5780
2	$C_{10}H_{21}$	3.04	2.989	0.051	−11.3230	−0.9590
3	$C_{11}H_{23}$	3.59	3.468	0.122	−7.9770	2.0180
4	$C_{12}H_{25}$	4.09	4.229	−0.139	−2.2290	6.2440
5	$C_{13}H_{27}$	4.63	4.643	−0.013	1.3400	8.0200
6	$C_{14}H_{29}$	4.82	4.915	−0.095	4.8020	7.8700
7	$C_{15}H_{31}$	5.14	4.908	0.232	7.0870	5.0780
8	$C_{16}H_{33}$	4.56	4.649	−0.089	7.2590	1.1260
9	$C_{17}H_{35}$	4.16	4.115	0.045	5.9850	−5.1030
10	$C_{18}H_{37}$	3.59	3.709	−0.119	4.7140	−9.4650
11	$C_{19}H_{39}$	3.61	3.552	0.058	4.2930	−11.2510
Red cell sheep. Log $C_{H_{50}}$: Eq. 11A						
1	C_8H_{17}	1.76	1.794	−0.034	−15.2830	−6.6450
2	$C_{10}H_{21}$	2.95	2.865	0.085	−9.2760	2.0000
3	$C_{12}H_{25}$	3.82	3.869	−0.049	−2.0040	6.9270
4	$C_{14}H_{29}$	4.40	4.448	−0.048	4.4230	5.4600
5	$C_{16}H_{33}$	4.79	4.715	0.075	10.0180	−0.2780
6	$C_{18}H_{37}$	4.52	4.550	−0.030	12.1220	−7.4650

model is excellent with relatively small standard deviations and high correlation coefficients. The press s's of these correlations are excellent considering the 'parabolic' or 'bilinear' nature of the correlations and the standard deviations of other equations from the parabolic or bilinear model. The single variable models account for 63–96% of the variance in the data depending on the nature of the microbial strains. The addition of the second latent variable explains 95–99.7% of the total variance in the data. The average standard deviation and the correlation coefficient of

TABLE 2
SUMMARY OF CoMFA, PARABOLIC [a], AND BILINEAR [b] MODELS

(1A–11A) CoMFA: Log BA[c] = a $Z1_{H_2O}$ + b $Z2_{H_2O}$ + c
(1B–11B) Parabolar: Log BA = a log P + b $(\log P)^2$ + c
(1C–11C) Bilinear: Log BA = a log P + b log (βP+1) + c

Eq.[d]	a	b	c	n	s	r	log P_o[e]
1A	0.059 (± 0.006)	0.012(± 0.004)	3.068 (± 0.034)	9	0.102	0.973	1.82
1B	0.55 (± 0.30)	−0.13 (± 0.07)	2.85 (± 0.26)	9	0.208	0.880	2.13
1C	0.766 (± 0.73)	−1.033(± 0.66)	2.866 (± 0.31)	9	0.168	0.937	1.56
2A	0.049 (± 0.003)	0.040(± 0.004)	4.300 (± 0.022)	10	0.071	0.993	2.32
2B	0.57 (± 0.18)	−0.12 (± 0.05)	4.08 (± 0.17)	10	0.183	0.949	2.38
2C	0.552 (± 0.20)	−0.937(± 0.30)	3.998 (± 0.15)	10	0.140	0.975	2.19
3A	0.048 (± 0.004)	0.043(± 0.005)	3.340 (± 0.031)	10	0.098	0.984	2.32
3B	0.78 (± 0.16)	−0.18 (± 0.04)	2.93 (± 0.15)	10	0.123	0.974	2.21
3C	0.675 (± 0.26)	−1.186(± 0.31)	2.878 (± 0.17)	10	0.132	0.974	2.10
4A	0.097 (± 0.005)	0.008(± 0.003)	3.223 (± 0.029)	10	0.090	0.989	2.32
4B	0.84 (± 0.23)	−0.21 (± 0.06)	2.94 (± 0.20)	10	0.172	0.960	1.97
4C	0.683 (± 0.29)	−1.439(± 0.35)	2.879 (± 0.19)	10	0.153	0.973	2.02
5A	0.064 (± 0.003)	0.063(± 0.004)	5.118 (± 0.022)	12	0.077	0.995	2.22
5B	0.90 (± 0.14)	−0.21 (± 0.04)	4.80 (± 0.14)	12	0.158	0.979	2.18
5C	1.047 (± 0.19)	−1.507(± 0.19)	4.757 (± 0.12)	12	0.100	0.993	1.79
6A	0.071 (± 0.003)	0.066(± 0.005)	4.410 (± 0.025)	12	0.088	0.995	2.82
6B	0.91 (± 0.21)	−0.17 (± 0.06)	3.87 (± 0.21)	12	0.230	0.966	2.68
6C	0.942 (± 0.26)	−1.274(± 0.31)	3.774 (± 0.18)	12	0.172	0.983	2.25
7A	0.077 (± 0.003)	0.057(± 0.003)	2.967 (± 0.022)	12	0.075	0.996	2.32
7B	0.93 (± 0.20)	−0.23 (± 0.05)	2.76 (± 0.20)	12	0.220	0.962	1.99
7C	0.983 (± 0.19)	−1.715(± 0.22)	2.643 (± 0.13)	12	0.122	0.990	1.86
8A	0.076 (± 0.002)	0.071(± 0.004)	4.384 (± 0.022)	12	0.075	0.997	2.82
8B	0.99 (± 0.17)	−0.19 (± 0.05)	3.80 (± 0.17)	12	0.190	0.980	2.65
8C	1.061 (± 0.20)	−1.376(± 0.23)	3.723 (± 0.14)	12	0.125	0.992	2.18
9A	0.109 (± 0.007)	0.081(± 0.012)	3.903 (± 0.067)	6	0.163	0.995	2.92
9B	1.26 (± 0.35)	−0.24 (± 0.11)	3.31 (± 0.37)	6	0.213	0.991	2.59
9C	2.139 (± 1.85)	−2.118(± 1.71)	3.871 (± 1.82)	6	0.171	0.996	–[f]
10A	0.082 (± 0.005)	0.069(± 0.006)	3.979 (± 0.038)	11	0.128	0.989	2.32
10B	1.34 (± 0.31)	−0.30 (± 0.08)	3.25 (± 0.28)	11	0.243	0.961	2.25
10C	1.150 (± 0.31)	−2.041(± 0.37)	3.159 (± 0.21)	11	0.170	0.984	2.16
11A	0.102 (± 0.003)	0.053(± 0.006)	3.707 (± 0.033)	6	0.081	0.998	2.92
11B	1.04 (± 0.14)	−0.16 (± 0.04)	3.05 (± 0.15)	6	0.084	0.998	3.15
11C	1.006 (± 0.50)	−1.191(± 0.95)	2.919 (± 0.40)	6	0.154	0.996	2.72

[a]Ref. 1.

[b]Ref. 2.

[c]1: *P. aeruginosa* (Log MIC); 2: *S. typhosa* (Log MIC); 3: *P. vulgaris* (Log MIC); 4: *P. vulgaris* (Log MKC); 5: *S. aureus* (Log MIC); 6: *Cl. welchii* (Log MIC); 7: *P. aeruginosa* (Log MKC); 8: *Cl. welchii* (Log MKC); 9: Red cell sheep (Log $C_{H_{50}}$); 10: *C. albicans* (Log MKC); Red cell sheep (Log $C_{H_{50}}$).

[d]1A: F = 52.3, P = 0.0002, press s = 0.161; 2A: F = 235.1, P = 0.0001, press s = 0.202; 3A: F = 104.9, P = 0.0001, press s = 0.267; 4A: F = 158.0, P = 0.0001, press s = 0.197; 5A: F = 443.0, P = 0.0001, press s = 0.206; 6A: F = 461.8, P = 0.0001, press s = 0.156; 7A: F = 511.6, P = 0.0001, press s = 0.198; 8A: F = 714.0, P = 0.0001, press s = 0.183; 9A: F = 149.1, P = 0.001, press s = 0.855; 10A: F = 188.1, P = 0.0001, press s = 0.277; 11A: F = 514.3. P = 0.0002, press s = 0.540.

[e]Log P_o values for the CoMFA model were estimated from 3D coefficient contour maps.

[f]Log P_o could not be determined.

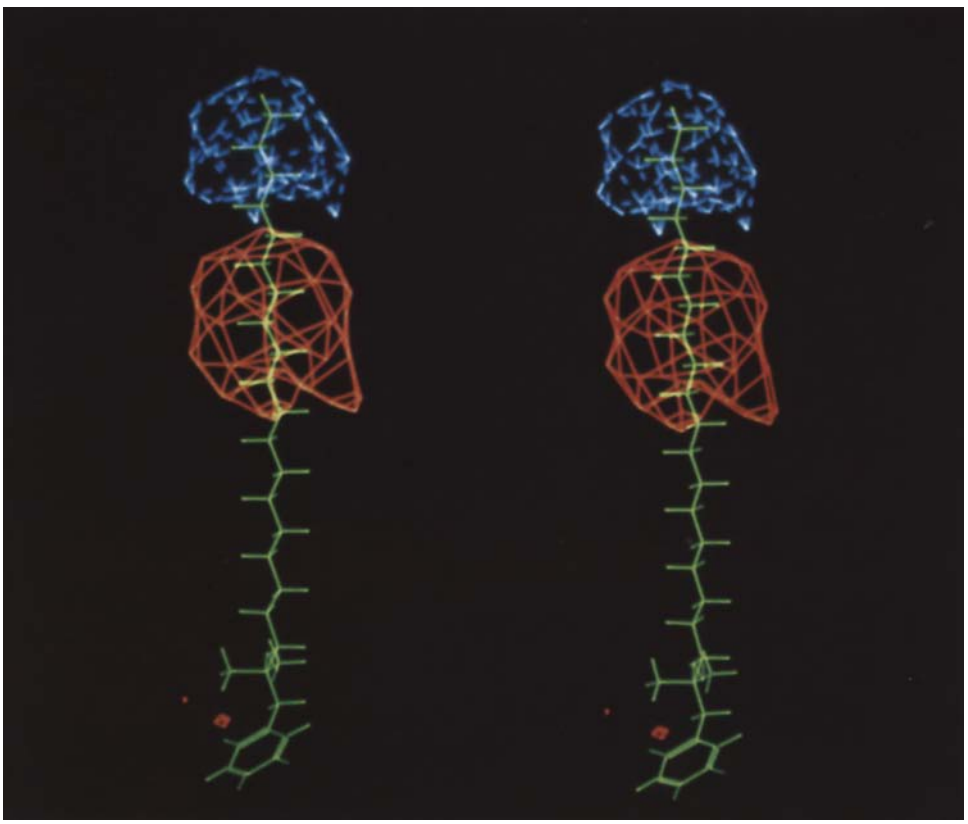

Fig. 1. Stereoscopic view of the major hydrophobic feature of Eq. 19. The positive contour region (in red) increases the antimicrobial potency and the negative contour region (in blue) decreases the potency. The nonadecyl analogue is used as a reference structure. (The contour is shown at 0.003 level.)

the CoMFA models are 0.095 and 0.990, respectively. In contrast, they are 0.184 and 0.964 for the parabolic models and 0.146 and 0.981 for the bilinear models.

Figure 1 is the coefficient contour plot of the correlation described in Eq. 7A*. The contour maps from other CoMFA models are not presented here, but they are similar to that of Eq. 7A. The area where hydrophobic substituents contribute positively towards increasing the antimicrobial potency is shown by the positive contour (in red), while the area where hydrophobic substituents contribute negatively is shown by the negative contour (in blue). Figure 2 is the plot between the observed and calculated log MIC values using Eq. 7A.

Table 1 lists the observed and calculated log MIC or log MKC values of the compounds included using Eqs. 1A–11A.

Equations 1–11 show that the molecular fields calculated with a H_2O probe produced correlations with an excellent standard error of estimate and a correlation coefficient compared to those

*Different contour levels show different degrees of the effects described by the positive and negative contours. The small patches of the contours in Fig. 1 are due to the small differences in the geometries and may be considered as noise.

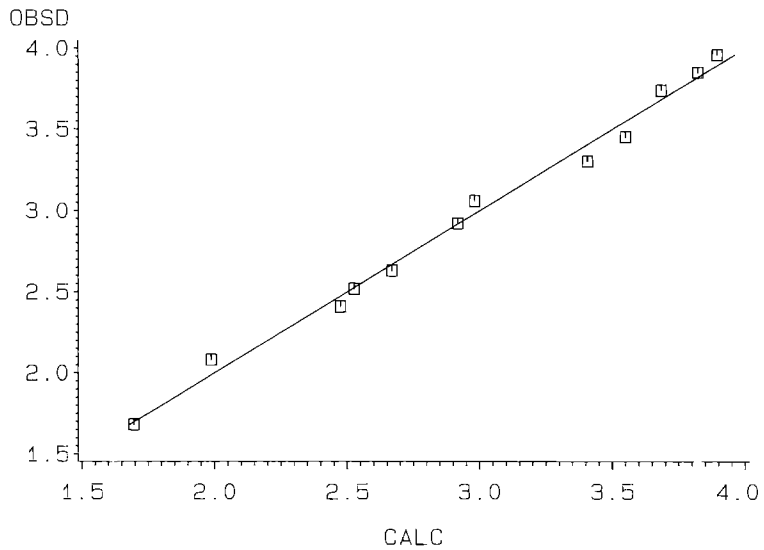

Fig. 2. Plot of observed vs. calculated log MKC using Eq. 7A.

with log P from the parabolic or bilinear model. The results demonstrate the applicability of the CoMFA methodology for describing nonlinear relationships in 3D QSAR.

DISCUSSION

In biological QSAR, nonlinear relationships between the lipophilicity of drugs and their activities are well known. Among the several models [3] that have been proposed to describe nonlinear relationships, the parabolic model and the bilinear model are used the most often.

The coefficient contour map of the nonlinear CoMFA models shows a characteristic pattern. Unlike the linear model where the positive or negative contours may prevail, depending on the sign of the coefficient, both contours are present and located next to one another in the nonlinear model. The positive contours correspond to the left side (ascending slope) of the optimum log P, while the negative contours correspond to the right side (descending slope) of the log P_o in the parabolic or bilinear model. Valuable information obtained from a parabolic or bilinear model is the optimum lipophilicity of the drug, log P_o. The usefulness of log P_o has been well demonstrated in the past [16,17]. In the present examples, where the substituents are *n*-alkyl groups, this information can be easily obtained from the CoMFA results. The region at the end of the positive contours appears to correspond to the optimum log P_o value *in these particular examples.* At present, the log P_o values are manually calculated from the coefficient contours*. Nonetheless,

*Because the structural variation is unidirectional, it was relatively simple to calculate the log P_o values in these examples. The log P_o values were calculated from the corresponding coefficient contours by first estimating the 'optimum' length of the 'alkyl' substituent, which corresponds to the end of the positive contour region toward the negative contour region. The log P_o value was then calculated by an interpolation for that optimum length of alkyl moiety from a linear plot of log P values for various *n*-alkyl groups. The calculated log MIC or MKC values were also compared in order to verify the proper selection of the optimum length of the alkyl substituent.

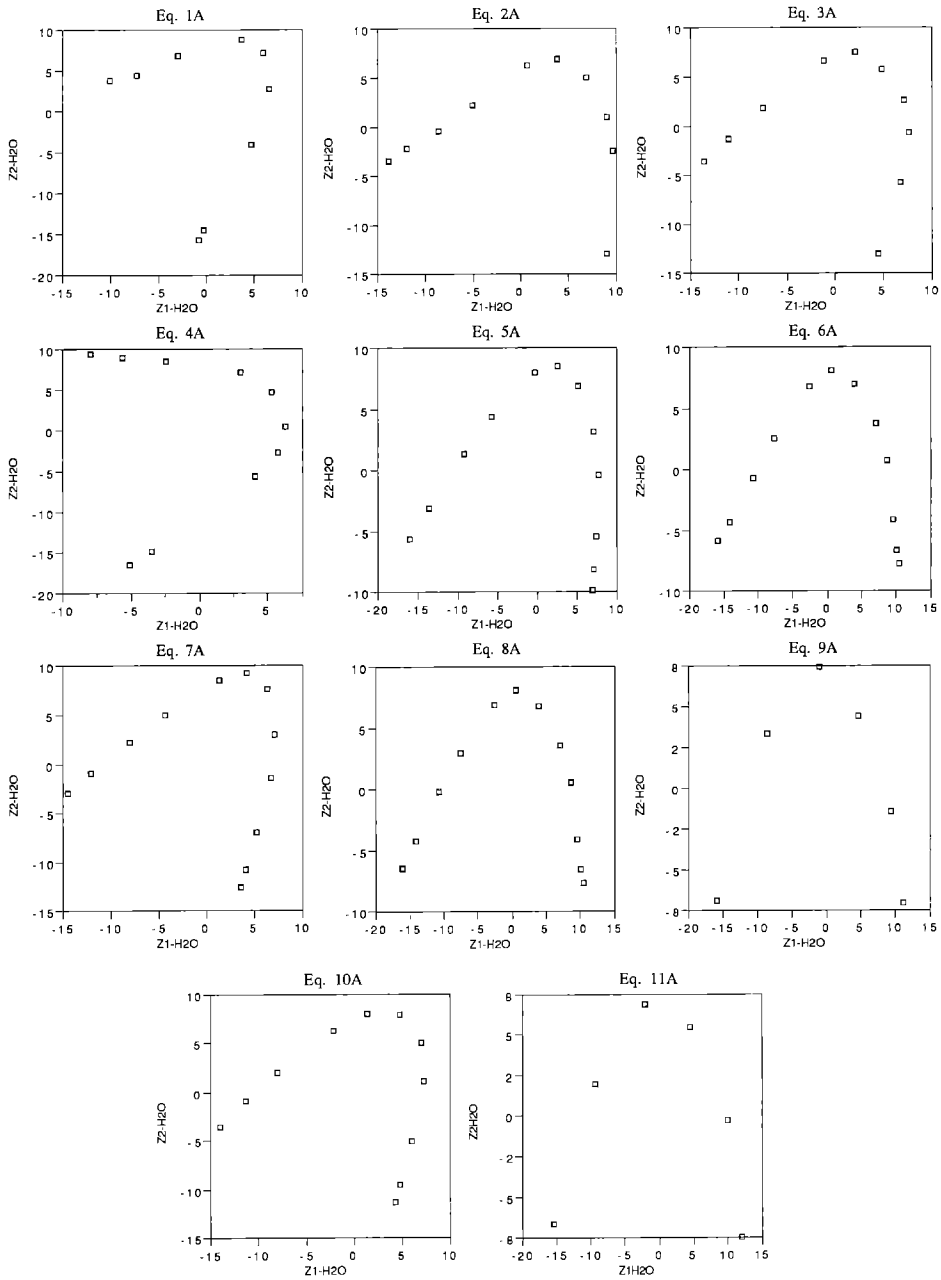

Fig. 3. Plots of the first ($Z1_{H_2O}$) and second ($Z2_{H_2O}$) latent variables from CoMFA models.

they are excellent compared to the optimum log P values from the parabolic or bilinear model and the real optimum in the observed biological activity.

Another characteristic in the nonlinear dependence of the biological activity is seen in the plots between the first and second latent variables ($Z1_{H_2O}$ and $Z2_{H_2O}$). Hellberg et al. [18] and Zalewski

[19] have previously utilized plots of the latent variables or principal components in the discussion of their studies. Figure 3 is a collection of the plots between $Z1_{H_2O}$ and $Z2_{H_2O}$ from Eqs. 1A–11A. It is interesting that these plots resemble a rotated 'parabolic' or 'bilinear' plot.

In traditional QSAR, it is preferred that the independent variables are orthogonal to each other in order for the regression analysis to give interpretable results. The presence of squared terms or cross terms usually leads to colinearities in the variables. The inclusion of highly correlated variables does not provide independent information for the regression analysis and may provide inconsistent and misleading results. In order to achieve good estimates of the regression coefficients, the independent variables must be relatively orthogonal to each other. Different authors have discussed this subject and proposed methods that can be used to make a linear variable and its square independent of each other [20,21]. In PLS, all the principal components are orthogonal to each other [19,22,23]. Therefore, there is no need for any special treatment to avoid such colinearity problems. This is one of the advantages in the CoMFA methodology and makes the CoMFA treatment of nonlinear cases even more attractive.

The effects of different lattice positions with respect to the molecules were investigated by translating the grid box in X, Y, and Z directions each by 0.5, 1.0, and 1.5 Å. Although not identical, the different lattice points gave results that are very similar. A larger number of excluded compounds (up to about 40%) in the jackknife cross-validation tests did not affect the cross-validation results.

Finally, the approaches described here for lipophilic dependence can be applied to the nonlinear dependence of other physicochemical properties, such as steric or electronic properties.

CONCLUSION

Several results are presented showing that the hydrophobic potential energy fields calculated with a H_2O probe with the GRID force field using a CoMFA approach produced significant correlations with excellent cross-validation. The results demonstrate the applicability of the CoMFA approach in describing nonlinear relationships in 3D QSAR studies.

REFERENCES

1 Hansch, C. and Clayton, J.M., J. Pharm. Sci., 62 (1973) 1.
2 Kubinyi, H., Arzneim.-Forsch. (Drug Res.), 26 (1976) 1991.
3 Kubinyi, H., QSAR in the Design of Bioactive Compounds. In Proceedings of the First International Telesymposium in Medicinal Chemistry, 18 February, 1984, J.R. Prous Publ., Barcelona, Spain, pp. 321–346.
4 Cramer, III, R.D., Patterson, D.E. and Bunce, J.D., J. Am. Chem. Soc., 110 (1988) 5959.
5 Kim, K.H. and Martin, Y.C., In Silipo, C. and Vittoria, A. (Eds.) QSAR: Rational Approaches on the Design of Bioactive Compounds (Proceedings of the 8th European Symposium, Sorrento (Napoli), Italy, 9–13 September, 1990), Elsevier, Amsterdam, 1991, pp. 151–154.
6 Kim, K.H. and Martin, Y.C., J. Org. Chem., 56 (1991) 2723.
7 Kim, K.H. and Martin, Y.C., J. Med. Chem., 34 (1991) 2056.
8 Kim, K.H., Med. Chem. Res., 1 (1991) 259.
9 GRID program, V7, Molecular Discovery Ltd., West Way House, Elms Parade, Oxford, U.K.
10 Rusinko, III, A., Skell, J.M., Balducci, R., McGarity, C.M. and Pearlman, R.S., The University of Texas at Austin and Tripos Associates, St. Louis, MO, 1988.
11 Liotard, D.A., Healy, E.F., Ruiz, J.M. and Dewar, M.J.S., AMPAC V 2.1 (QCPE No. 506). Ran with the keywords NOINTER and XYZ.

12 Lindberg, W., Persson, J.-A. and Wold, S., Anal. Chem., 55 (1983) 643.
13 Cramer, III, R.D., Brunce, J.D., Patterson, D.E. and Frank, I.E., Quant. Struct.-Act. Relat., 7 (1988) 18.
14 Cutler, R.A., Cimijotti, E.B., Okolowich, T.J. and Wetterau, W.F., Chem. Spec. Mfr. Ass., Proc. Annu. Meet., 53 (1966) 102.
15 Kubinyi, H., J. Med. Chem., 20 (1977) 625.
16 Hansch, C., Bjorkroth, J.P. and Leo, A., J. Pharm. Sci., 76 (1987) 663.
17 Hansch, C., Kim, D., Leo, A.J., Novellino, E., Silipo, C. and Vittoria, A., CRC Crit. Rev. Toxicol., 19 (1989) 185.
18 Hellberg, S., Wold, S., Dunn, III, W.J., Gasteiger, J. and Hutchings, M.G., Quant. Struct.-Act. Relat., 4 (1985) 1.
19 Zalewski, R.I., In Zalewski, R.I., Krygowski, T.M. and Shorter, J. (Eds.) Similarity Models in Organic Chemistry, Biochemistry and Related Fields, Elsevier, Amsterdam, 1991, p. 455.
20 Berntsson, P., Acta Pharm. Suec., 17 (1980) 199.
21 Goodford, P.J., Adv. Pharmacol. Chemother., 11 (1973) 51.
22 Dunn, III, W.J., Wold, S., Edlund, U., Hellberg, S. and Gasteiger, J., Quant. Struct.-Act. Relat., 3 (1984) 131.
23 Glen, W.G., Dunn, III, W.J. and Scott, D.R., Tetrahed. Comput. Methodol., 2 (1989) 349.

APPENDIX

CARTESIAN COORDINATES OF NONADECYL ANALOGUE

C1	10.000	8.539	1.175
C2	10.450	9.858	1.159
C3	10.689	10.504	−0.055
C4	10.455	9.834	−1.258
C5	9.945	8.538	−1.247
C6	9.689	7.895	−0.029
C7	9.095	6.527	−0.017
N8	7.574	6.529	0.037
C9	7.028	7.260	−1.140
C10	7.115	7.193	1.289
C11	7.106	5.093	0.012
C12	5.593	4.919	−0.002
C13	5.231	3.446	0.026
C14	3.724	3.297	−0.003
C15	3.295	1.845	−0.004
C16	1.784	1.751	−0.016
C17	1.303	0.316	−0.005
C18	−0.210	0.265	−0.017
C19	−0.726	−1.158	0.003
C20	−2.240	−1.177	−0.006
C21	−2.783	−2.589	0.000
C22	−4.297	−2.588	−0.009
C23	−4.853	−3.996	0.002
C24	−6.367	−3.983	−0.006
C25	−6.852	−5.366	0.013
C26	−8.365	−5.415	0.008
C27	−8.868	−6.843	0.024
C28	−10.380	−6.895	0.005
C29	−10.882	−8.316	0.021